Targeted Insertion of the Cre-Recombinase Gene at the Phenylethanolamine n-Methyltransferase Locus: A New Model for Studying the Developmental Distribution of Adrenergic Cells

Steven N. Ebert,[1]* Qi Rong,[1] Steven Boe,[2] Robert P. Thompson,[3] Alexander Grinberg,[2] and Karl Pfeifer[2]

To evaluate the developmental distribution of adrenergic cells in vivo, we inserted the Cre-recombinase gene into the locus encoding for the epinephrine biosynthetic enzyme phenylethanolamine n-methyltransferase (Pnmt) and crossed these Pnmt-Cre mice with ROSA26 reporter (R26R) mice to activate LacZ (encoding β-galactosidase) expression in cells that were selectively derived from the adrenergic lineage. Our data show the following: (1) Insertion of Cre-recombinase into the Pnmt locus created a functional knockout of Pnmt expression with concomitant loss of epinephrine in homozygous $Pnmt^{Cre/Cre}$ mice; (2) Despite the reduction in Pnmt expression and epinephrine production in $Pnmt^{Cre/Cre}$ mice, these mice were viable and fertile, with no apparent developmental defects; (3) When crossed with R26R mice, Pnmt-Cre activation of LacZ expression faithfully recapitulated Pnmt expression in vivo; and (4) LacZ expression was activated in substantial numbers of pacemaking, conduction, and working cardiomyocytes. ***Developmental Dynamics 231:849–858, 2004.*** **© 2004 Wiley-Liss, Inc.**

Key words: epinephrine; catecholamines; pacemaking; heart development

Received 7 May 2004; Revised 6 July 2004; Accepted 14 July 2004

INTRODUCTION

Epinephrine (EPI) and norepinephrine (NE) are the major peripheral catecholamines produced in mammals. They are synthesized by means of the enzymatic conversion of dopamine to NE by the action of dopamine β-hydroxylase (Dbh) and, subsequently, of NE to EPI by the action of phenylethanolamine n-methyltransferase (Pnmt; Cooper et al., 1991). In adult mammals, this synthesis occurs primarily in the adrenal medulla and in the sympathetic nervous system. Mice that lack the ability to produce NE and EPI due to targeted disruption of the Dbh gene die in utero from apparent cardiac failure (Thomas et al., 1995).

The vast majority of $Dbh^{-/-}$ mouse embryos die before the adrenal gland even forms and before maturation of the sympathetic nervous system, suggesting that the primary source(s) of catecholamine biosynthesis in the embryo must be different from that in adult mice (Thomas et al., 1995). One potential source is the heart itself, where we and others have shown that intrinsic cardiac adrenergic (ICA) cells are present beginning at relatively early stages (embryonic day (E) 9.5 in rat; E3 in chick) of cardiac development (Ignarro and Shideman, 1968; Ebert et al., 1996; Huang et al., 1996; Ebert and Thompson, 2001). A specific developmental role for these ICA cells remains elusive, but we have shown recently that they are transiently and progressively associated with regions of the heart that become pacemaking and conduction tissue (Ebert and Thompson, 2001). This association was initially observed in the

[1]Department of Pharmacology, Georgetown University Medical Center, Washington, DC
[2]Laboratory of Mammalian Genes and Development, NICHD/NIH, Bethesda, Maryland
[3]Department of Cell Biology and Anatomy, Medical University of South Carolina, Charleston, South Carolina
Grant sponsor: Georgetown University Medical Center; Grant sponsor: Stem Cell Research Foundation (a program of the American Cell Therapy Research Foundation); Grant sponsor: National Institute of Child Health and Development.
*Correspondence to: Steven N. Ebert, Ph.D., Department of Pharmacology, Georgetown University Medical Center, 3900 Reservoir Road, NW, Washington, DC 20057. E-mail: eberts@georgetown.edu

DOI 10.1002/dvdy.20188
Published online 29 October 2004 in Wiley InterScience (www.interscience.wiley.com).

sinoatrial node (SAN) and atrioventricular canal regions at approximately E11.5 in the rat. The clustering of ICA cells in these regions then declined over the next several days of development but reappeared along the crest of the ventricular septum (bundle of His region) and, somewhat more sporadically, trailing down the ventricular septum toward the apex at approximately E16.5 (Ebert and Thompson, 2001). These patterns of ICA cell distribution were transient, lasting not more than 1–2 days in each of these locations (Ebert and Thompson, 2001). It was not clear if this progressive appearance and disappearance of ICA cells in these various cardiac regions was due to migration, differentiation, and/or death of ICA cells.

To help resolve these possibilities, we have developed a novel mouse genetic model. The Cre-recombinase gene was inserted into the endogenous Pnmt locus (Pnmt-Cre) so that Cre-recombinase expression would be directed by Pnmt regulatory DNA sequences. Upon crossing these Pnmt-Cre mice to the reporter R26R strain of mice, we anticipated activation of LacZ expression exclusively in adrenergic cells by means of Cre-mediated recombination of upstream loxP sites flanking a DNA sequence responsible for blocking transcription of the LacZ gene (Soriano, 1999). In this system, lacZ expression does not require the continuous activation of Pnmt-Cre. Rather, the genetic changes induced at the Rosa26 locus by transient expression of the Cre-recombinase permanently mark the altered cells and their descendants as β-galactosidase positive and, therefore, provide a means to follow the distribution of adrenergic-derived cells throughout development. In addition, because the targeted insertion of Cre-recombinase disrupted the expression of the Pnmt gene, we could assess the potential consequences of selective adrenergic deficiency in these mice.

RESULTS

To determine whether epinephrine plays an important role during development and to identify adrenergic cell descendants in the developing mouse, we inserted the Cre-recombinase gene into the mouse Pnmt locus so the expression of Cre-recombinase would be dependent upon Pnmt regulatory sequences (Fig. 1A). Specifically, we inserted the Cre-recombinase gene into exon 1, creating a gene fusion of the 5′ leader sequences from Pnmt directly to Cre-recombinase open reading frame. This strategy was designed to disrupt functional expression of Pnmt while permitting expression of Cre-recombinase exclusively in adrenergic cells. Verification of the correct targeting of the Cre-recombinase insert was confirmed by Southern blotting using 5′ and 3′ probes each external to the targeting vector (Fig. 1B).

Two of the correctly targeted clones were further propagated and introduced into mouse blastocysts, and independent lines of founder mice were produced. These founder mice were crossed with wild-type C57B/6 females to generate F1 animals used in all our subsequent studies. Germ-line transmission of the Pnmt-Cre allele was verified initially by Southern blotting and then by polymerase chain reaction (PCR; Fig. 1C). When F1 heterozygotes were intercrossed, mice harboring the disrupted Pnmt allele were born in normal Mendelian ratios. 35 +/+: 75 +/−: 46 −/− were the actual numbers of mice born as compared with 39, 78, and 39 mice expected for each genotypic class from 156 total progeny ($P = 0.410$ using the Chi−squared test). The −/− mice appear overtly normal and are fertile even in −/− × −/− crosses.

The absence of Pnmt expression was predicted to result in mice that cannot produce epinephrine. To test this hypothesis, we measured EPI and NE concentrations in adrenal extracts from $Pnmt^{+/+}$, $Pnmt^{+/Cre}$, and $Pnmt^{Cre/Cre}$ mice by radioimmunoassay (Table 1). EPI was not detectable in extracts from $Pnmt^{Cre/Cre}$ mice, and the concentration of NE was found to be significantly greater in $Pnmt^{Cre/Cre}$ relative to $Pnmt^{+/+}$ and $Pnmt^{+/Cre}$ extracts ($P < 0.001$). In contrast, NE and EPI concentrations were similar in extracts from $Pnmt^{+/+}$ and $Pnmt^{+/Cre}$ mice. In addition, Pnmt immunofluorescent histochemical staining was virtually absent in the adrenal medullae of $Pnmt^{Cre/Cre}$ mice but could be readily detected in $Pnmt^{+/Cre}$ and $Pnmt^{+/+}$ mice (data not shown).

To map the developmental distribution of Pnmt-Cre–expressing cells and their descendants, mice heterozygous for the insertion ($Pnmt^{+}$/Cre) were mated with R26R mice, homozygous at the ROSA26 reporter locus. Cells in R26R mice have the ability to robustly express the bacterial LacZ (β-galactosidase) gene if activated by Cre-recombinase (due to removal of a floxed transcriptional block; Soriano, 1999). To determine whether our system was working, we first examined β-galactosidase staining in adrenal glands where the expression patterns of Pnmt are well-documented and relatively simple. As illustrated in Figure 2A, Pnmt immunofluorescent staining is concentrated in the adrenal medulla. An adjacent section stained with XGAL to detect LacZ expression (blue cells) produced a nearly identical pattern of staining (Fig. 2B). When Pnmt immunofluorescent staining was performed on this section after the XGAL staining, little or no fluorescently stained cells were observed, because the XGAL blocked or quenched the fluorescence in costained cells (Fig. 2C). Thus, the localization of Pnmt and β-galactosidase appear to be completely coincident here. As a control, the same sections were also stained for tyrosine hydroxylase (Th), the first enzyme in the catecholamine biosynthetic pathway, to independently identify chromaffin cells (Fig. 2D–F). As expected, Th staining was similar to Pnmt and XGAL staining in these sections, but there were a few cells that stained positively for Th that were not stained with XGAL (Fig. 2E,F, arrows). These $Th^{+}LacZ^{-}$ cells presumably represent the minority of chromaffin cells that are known to be noradrenergic rather than the adrenergic majority (Coupland and Tomlinson, 1989; Ebert and Thompson, 2001). Together, these results demonstrate that LacZ expression was highly selective in adrenal sections where it

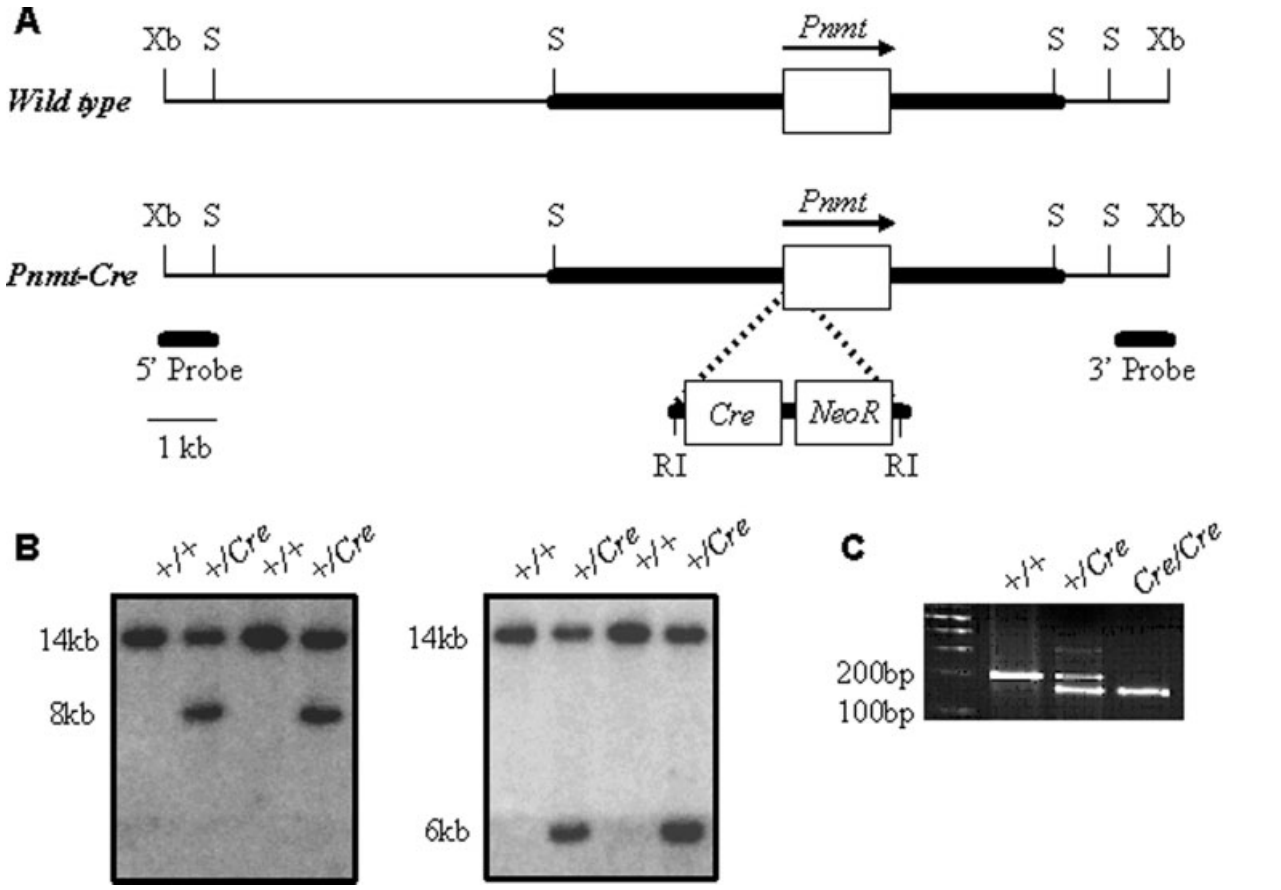

Fig. 1. Construction and verification of the Pnmt-Cre allele. (The Cre-recombinase gene was inserted into the endogenous phenylethanolamine n-methyltransferase locus (Pnmt-Cre).) **A:** Cartoon depiction of the wild-type and Pnmt-Cre alleles. Sequences coding for the Pnmt RNA are depicted as an open rectangle with the direction of transcription indicated by the arrow. The thickened line shows the Pnmt sequences used to direct the homologous recombination event that introduces the Cre-recombinase gene (Cre) and the Neomycin resistance gene (NeoR) into Pnmt exon 1. Cre-recombinase is fused to the Pnmt 5′ untranslated region sequences so that its transcription is entirely dependent upon Pnmt regulatory elements. The Cre insert contains transcriptional stop sequences. NeoR is driven by its own promoter and the NeoR gene is flanked with Frt sites to allow its removal by means of Flp recombinase. The 5′ and 3′ probes used for verifying the alleles are depicted. **B:** Southern analysis of the mutated cell lines identifies clones carrying the Pnmt-Cre insertion allele. When digested with *Xba*I and *Eco*RI, correctly targeted cells display an 8-kb band (5′ probe/left panel) or a 6-kb band (3′ probe/right panel) in addition to the 14-kb band indicative of the wild-type chromosome. **C:** Polymerase chain reaction analysis described in the Experimental Procedures section distinguishes homozygous wild-type (+/+), heterozygous mutant (+/Cre), and homozygous mutant (Cre/Cre) animals. RI, *Eco*RI; S, *Sac*I; Xb, *Xba*I.

TABLE 1. Adrenal Catecholamine Content (pg/ng protein)[a]

Genotype	NE	EPI
$Pnmt^{+/+}$ (n = 5)	14.2 ± 0.6	24.6 ± 2.9
$Pnmt^{+/Cre}$ (n = 10)	17.8 ± 1.4	25.0 ± 2.8
$Pnmt^{Cre/Cre}$ (n = 4)	32.8 ± 2.6[b]	< 0.004[b]

[a]Pnmt, phenylethenolamine n-methyl transferase; NE, norepinephrine; EPI, epinephrine.
[b]$P < 0.001$ compared to $Pnmt^{+/+}$ and $Pnmt^{+/Cre}$

was confined to adrenergic ($Pnmt^{+}$) cells.

To evaluate Pnmt-Cre expression in the developing mouse embryo, we performed whole-mount staining with XGAL. The earliest stage of development when LacZ expression could be detected was E8.5. LacZ expression was observed in the heart (Fig. 3A) and along the dorsal ridges of the neural folds in the region of the midbrain–hindbrain junction (Fig. 3B). Within the heart, there appears to be a small cluster of $LacZ^{+}$ cells in the sinus venosus region (Fig. 3A, arrow), with a few additional $LacZ^{+}$ cells apparent in the ascending loop and also near the atrioventricular junction (see arrowheads, Fig. 3A).

Over the next 2 days, LacZ expres-

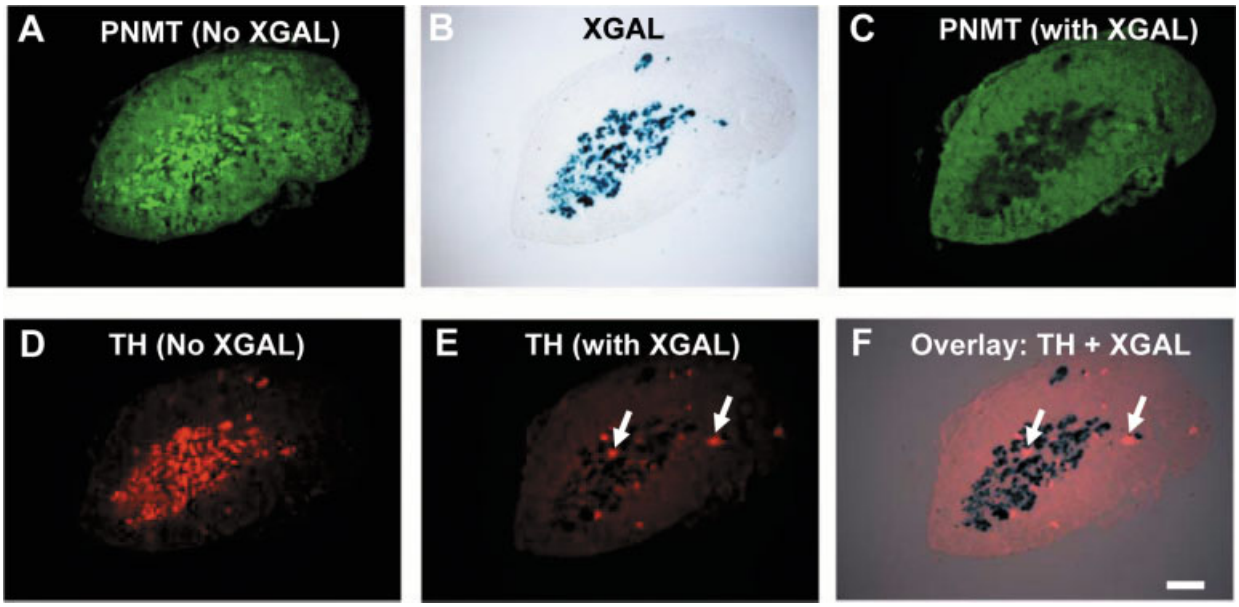

Fig. 2.

sion became much more widespread in the heart, as shown in Figure 4A. By this time, LacZ expression was also evident in the brainstem region, 2nd branchial arch, and sporadically along the dorsal surface of the embryo. LacZ expression was dependent upon Cre-recombinase expression from the Pnmt locus, because none was observed when wild-type embryos were similarly crossed with R26R mice (Fig. 4B).

Although it appears from the whole-mount staining (Fig. 4A) that the entire heart was expressing LacZ at this stage of development, examination of heart sections from these embryos revealed that the true staining pattern was more restricted (Fig. 5). Sporadic staining of cardiac cells was observed in the atrial and ventricular regions, including cells in the trabecular region of the ventricle. As shown in Figure 5, LacZ expression was observed in the SA junction region (Fig. 5A,B); however,

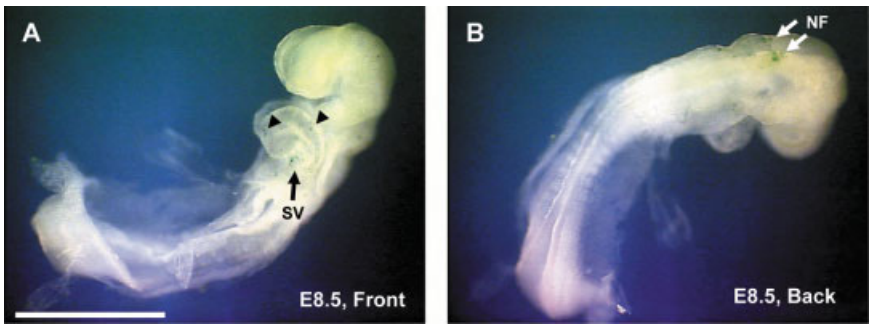

Fig. 3.

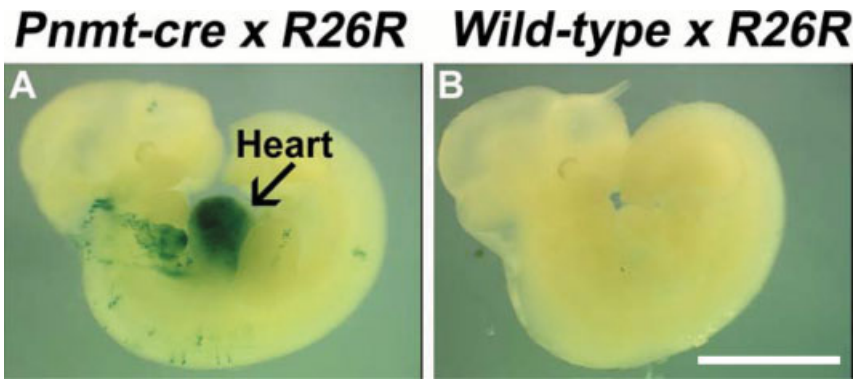

Fig. 4.

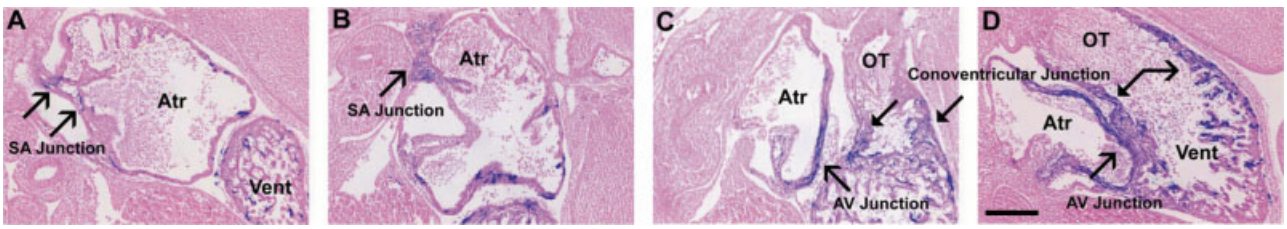

Fig. 5.

the strongest LacZ staining was found near the antrioventricular and conoventricular junction regions (Fig. 5C,D). These LacZ expression patterns were consistently observed at this stage of development, and they appear similar to the pattern of catecholamine-producing cells previously reported at a comparable developmental stage in the rat (Ebert and Thompson, 2001).

The pattern of LacZ expression in the heart appears to be restricted to myocardial cells. To further evaluate this observation, we performed triple-labeling experiments whereby Pnmt-Cre/R26R heart sections (E9.5) were stained for expression of (1) a muscle-specific marker, sarcomeric α-actinin (red fluorescence, Fig. 6A), (2) LacZ as a marker for cells descended from an adrenergic lineage (blue XGAL staining, Fig. 6B), and (3) the adrenergic cell marker Pnmt (green fluorescence, Fig. 6C). Extensive overlap of these three staining patterns could be observed by merging the individual staining panels into a single "overlay" image, as shown in Figure 6D. The yellow regions represent cells that coexpress α-actinin and Pnmt (arrows point to some examples of overlapping expression patterns). Some cells are clearly red or green, but many yellow cells can also been seen in this image. Notably, most of the exclusive green ($Pnmt^+/\alpha\text{-actinin}^-$) cells in the overlay image (Fig. 6D) were found just outside the heart, in both the anterior region adjacent to the outflow tract as well as in the posterior region adjacent to the atrial chamber (indicated by the arrowheads, Fig. 6C,D). The $LacZ^+$ cells (blue) were again found concentrated at junction regions, specifically between the atrial, ventricular, and outflow tract cavities.

By E15.5, the heart has matured morphologically to assume its adult-like appearance. To determine whether Pnmt-expressing cells contribute to pacemaker cells in the SAN, we performed a preliminary immunofluorescent histochemical staining analysis of wild-type E15.5 mouse embryo sections using an antibody that recognizes the *Hyperpolarization-activated cyclic nucleotide-modulated channel isoform 4* (HCN4), a major pacemaker channel protein expressed in the SAN (Garcia-Frigola et al., 2003; Stieber et al., 2003). As shown in Figure 7A, HCN4 staining is highly restricted to the SAN region of the right atrium (arrow) and to a lesser extent, to the atrioventricular node (AVN) region (arrowhead). In contrast, sarcomeric α-actinin was found to be expressed throughout the myocardium in this section (Fig. 7B). These data confirm that HCN4 was localized to pacemaker cells in the developing mouse heart.

As shown in the series of sections from a Pnmt-Cre/R26R embryo, LacZ expression not only persists in the heart at E15.5 but is highly pervasive throughout the myocardium in all four chambers (Fig. 7C–E). By far, the strongest and most extensive labeling was found in the ventricular septum, with the most prominent staining appearing at the crest of the septum and extending laterally into both ventricular chambers along the base as well as caudally down the septum toward the apex. LacZ expression in the free walls of both chambers was considerably more sparse than that found in the septum, with a tendency to be localized in cells near the endocardial surface, although $LacZ^+$ cells were also clearly seen in the mid- and epicardial regions of the ventricular myocardium. There appeared to be little or no LacZ expression in the aorta, aortic valves, and mitral valves, all of which can be clearly seen as nonstained tissue in Figure 7D; however, the myocardial region immediately adjacent to the intake region of each of these valves was strongly labeled with blue XGAL stain.

Within the atria, LacZ expression was sporadic, with the majority of atrial myocytes appearing as nonstained cells. The exception to this pattern of atrial staining appeared in the SAN region where a strong clustering of blue $LacZ^+$ cells was evident (Fig. 7E,F). To show that these cells were SAN myocytes, we performed immunofluorescent histochemical staining of the sections with the anti-HCN4 antibody. As shown in Figure 7G,H, HCN4 expression is robust in this region and overlaps extensively with the XGAL staining. These results demonstrate that many, but not all, of the presumptive pacemaker cells ($HCN4^+$) in the SAN also expressed LacZ in these Pnmt-Cre/R26R mice.

Although LacZ expression is found in pacemaker cells, as we have just shown, it is clear from the data pre-

Fig. 2. Coimmunofluorescent and XGAL histochemical staining in neonatal adrenal sections in Pnmt-Cre/R26R mice. **A:** PNMT immunofluorescent histochemical staining (fluorescein isothiocyanate filters). **B:** Adjacent section stained with XGAL. **C:** PNMT immunofluorescent histochemical staining of the section shown in B after XGAL staining. Note that the XGAL staining blocks the fluorescent signal in costained cells. **D:** Tyrosine hydroxylase (TH) immunofluorescent histochemical staining (Texas Red filter) of the same section as shown in A. **E:** TH immunofluorescent histochemical staining of an adjacent section (same section as shown in B,C) after XGAL staining. **F:** Overlay of images in D and E showing TH immunofluorescence and XGAL staining simultaneously. Arrows in E and F indicate examples of TH^+ cells that were not stained with XGAL. Scale bar = 0.1 mm in F (applies to A–F). PNMT, phenylethanolamine n-methyltransferase.

Fig. 3. Whole-mount XGAL staining of an embryonic day (E) 8.5 Pnmt-Cre/R26R embryo. **A:** Left ventral view. Arrow points to $LacZ^+$ blue-stained cells in the sinus venosus (SV) region. Arrowheads indicate positions of additional $LacZ^+$ cells in this heart. **B:** Right dorsal view. Arrows point to $LacZ^+$ blue-stained cells along the dorsal crest of the neural folds (NF).

Fig. 4. Whole-mount XGAL staining in embryonic day (E) 10.5 mouse embryos. **A,B:** Pnmt-Cre/Pnmt+, R26R/+ (A) and Pnmt+/Pnmt+, R26R/+ (B) mouse embryos at E10.5. Right sagittal views are shown. The arrow depicts the heart. Staining can also be seen in the brainstem and 2nd branchial arch regions. Sparse patches of XGAL staining are also seen along the back (dorsal surface) and in the forelimb of the Pnmt-Cre x R26R embryo. Scale bar = 1.0 mm in B (applies to A,B).

Fig. 5. Identification of $LacZ^+$ cells in embryonic day (E) 10.5 mouse heart sections. **A–D:** Series of sagittal sections from left to right through an E10.5 heart from a Pnmt-Cre/R26R embryo that was stained with XGAL and counterstained with eosin are shown. Arrows depict areas of the heart that were stained blue with XGAL. Atr, atrial chamber; AV, antrioventricular; OT, outflow tract SA, sinoatrial; Vent, ventricular chamber; Pnmt, phenylethanolamine n-methyltransferase. Scale bar = 0.1 mm in D (applies to A–D).

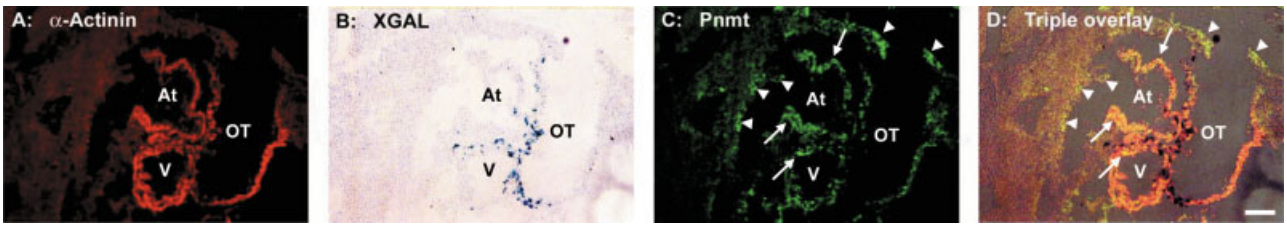

Fig. 6. Coimmunofluorescent and XGAL histochemical staining in an embryonic day (E) 9.5 Pnmt-Cre/R26R mouse heart. The same section is shown in A–D (right sagittal view). **A:** Sarcomeric α-actinin, a myocyte-specific marker, is visualized as Texas Red fluorescent staining. **B:** Brightfield image depicting LacZ^{+} cells (stained blue with XGAL). **C:** Pnmt, an ICA cell marker, is seen as green (fluorescein isothiocyanate) fluorescent staining. **D:** Overlay image showing all three staining patterns simultaneously. Yellow regions represent apparent costaining for sarcomeric α-actinin and Pnmt (arrows). The arrowheads depict regions of the embryo that were stained exclusively for Pnmt. Pnmt, phenylethanolamine n-methyltransferase. Scale bar = 0.1 mm in D (applies to A–D).

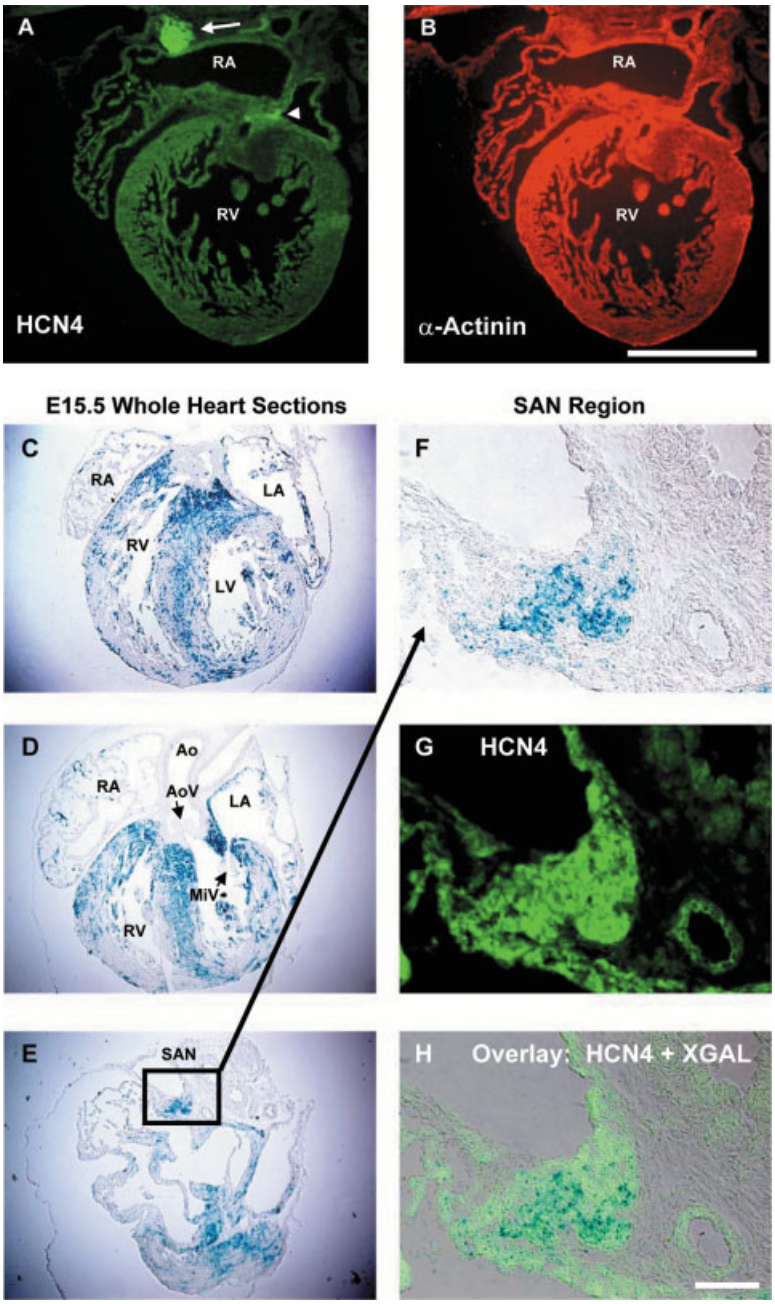

Fig. 7. Pnmt-Cre expression in the sinoatrial node (SAN) region of embryonic day (E) 15.5 mouse hearts. **A,B:** Coimmunofluorescent histochemical staining of wild-type (Pnmt$^{+/+}$) E15.5 mouse heart sections for HCN4 (an arrow depicts SAN myocytes, and an arrowhead indicates presumptive atrioventricular node myocytes, A), and sarcomeric α-actinin (B). RA, right atrium; RV, right ventricle. **C–H:** Frontal series of E15.5 Pnmt-Cre/R26R heart sections stained for expression of LacZ (C–F) and the pacemaker channel protein, HCN4 (G,H). An expanded view of the boxed region (SAN) in E is shown in F. G: Upon switching to darkfield fluorescence microscopy with fluorescein isothiocyanate filters, HCN4 staining can be seen in this section. To evaluate costaining for XGAL and HCN4 in this section, the images in F and G were combined to produce the overlay image depicted in H. Ao, aorta, AoV, aortic valve, MiV, mitral valve; pnmt, phenylethanolamine n-methyltransferase. Scale bars = 1.0 mm in B (applies to A–E), 0.1 mm in F–H.

sented thus far that LacZ expression in the heart extends well beyond the SAN region. By E15.5, most of the LacZ-expressing cells are found throughout the myocardium, as indicated above (see Fig. 7C–E).

This pattern of LacZ expression persisted in the heart through at least the early postnatal period. As shown in Figure 8, extensive XGAL labeling was observed throughout the heart, and was especially dense in the ventricular septum. Many of the pacemaker cells ($HCN4^+$) were also stained blue with XGAL (Fig. 8B–D). Endogenous Pnmt expression in the SAN region was extremely weak at this stage of development (Postnatal day 2, P2), being at best confined to a small cluster of cells (see arrowhead, Fig. 8E).

DISCUSSION

EPI-Deficient Mice Appear Normal

In this report, we have described the initial characterization of a novel mouse model for studying adrenergic cell function and distribution. Targeted disruption of the Pnmt gene led to the production of mice that were deficient in their ability to produce EPI. These mice were still able to produce NE. Thus, these mice are a model for investigating the specific role of epinephrine in mouse biology.

There was no overt developmental phenotype associated with EPI deficiency in that homozygous mice lacking EPI survived to adulthood, were physically indistinguishable from wild-type and heterozygous littermates, and were able to breed effectively. We have not as yet explored more subtle physiological or behavioral phenotypes in these mice, but one might expect that they may have limitations in their ability to mediate stress responses, because EPI is one of the primary physiological "stress" hormones.

Mapping Adrenergic Cells and Their Descendants

The earliest expression of LacZ in Pnmt-Cre/R26R mice occurred around E8.5 in the region of the neural folds and in the heart. This essentially simultaneous activation of LacZ in these two disparate regions of the embryo suggests that adrenergic cells arise independently from neural and cardiac precursors. A neural origin for adrenergic cells is well-established in the literature, as Pnmt-expressing adrenal chromaffin cells are known to be derived from neural crest (Bohn, 1983; Anderson, 1993). In addition, Pnmt-expressing cells are also known to contribute to specific populations of brainstem and retinal neurons (Kopp et al., 1979; Armstrong et al., 1982; Bohn et al., 1986; Sawchenko and Bohn, 1989; Hammang et al., 1992). We did not examine the retina in this study, but we did show that $LacZ^+$ cells were present in the brainstem region as early as E8.5 (Fig. 3). We have also observed $LacZ^+$ cells in the neonatal brainstem (not shown). Taken together, the $LacZ^+$ staining patterns in the developing embryo and neonate are consistent with a neurogenic origin of these cells in the brain and adrenal gland.

In contrast, $Pnmt^+$ cells in the heart appear to have a cardiogenic rather than a neurogenic origin, because they appear independently in the heart and neural fold regions by E8.5. In support of this hypothesis, we demonstrated that Pnmt-expressing cells were found in the presumptive posterior and anterior heart-forming regions at E9.5 (Fig. 6). Although it is generally well-accepted that the vast majority of myocardial cells arise "from paired heart-forming fields at the venous pole" (Kelly and Buckingham, 2002), several recent studies from independent laboratories have shown that there is also an anterior (arterial) pole from which myocardial cells are derived (Waldo et al., 2001; Mjaatvedt et al., 2001; Kelly et al., 2001). As was suggested from early data published in the 1970s (Viragh and Challice, 1973; de la Cruz et al., 1977), myocardial cells derived from the anterior heart-forming region primarily populate and extend the outflow tract. Kelly et al. (2001) showed that at least part of the anterior heart-forming field emanated from the pharyngeal arch region between E8.25 and E10.5 in the mouse. Our data identified $LacZ^+$ cells in the pharyngeal arch region during that window of development and showed that many adrenergic-derived myocardial cells were present in the developing outflow tract. These data suggest that adrenergic cells contribute to myocardial development from the anterior as well as the posterior heart-forming fields. Pnmt expression in extracardiac (α-actinin–negative) cell populations at both poles of the tubular heart may indicate expression of Pnmt just before commitment to the myocardial phenotype, a potentially important observation in light of earlier studies (Claycomb, 1976, 1977; Hoffman, 2001), or merely differential sensitivity of these two antibodies as applied here. Although there may be some contributing $Pnmt^+$ cells derived from neural crest in the heart after approximately E10.5, the LacZ staining patterns reported here are not consistent with established cardiac neural crest patterns in the developing heart (Waldo et al., 1999; Kirby, 1999; Jiang et al., 2000). Clearly, further work is needed to resolve this issue and to definitively determine whether the adrenergic lineage hypothesis of cardiomyocyte development proposed here is valid.

Pnmt-Expressing Cells Become Pacemaking and Conduction System Myocytes

We previously showed that ICA cells were transiently and progressively associated with pacemaking and conduction system regions (SAN, AVN, bundle of His, and Purkinje fibers) within the embryonic rat heart (Ebert and Thompson, 2001). The results from the present study in the mouse confirm and extend these findings by showing that a subset of pacemaking cells in the SAN and AVN were derived from adrenergic cells because approximately half of the pacemaker myocytes that stained positively for the pacemaker channel protein, HCN4, also stained positively with XGAL. Although we do not have an antibody marker that selectively recognizes His bundle or Purkinje fiber myocytes, the extensive XGAL labeling of the ven-

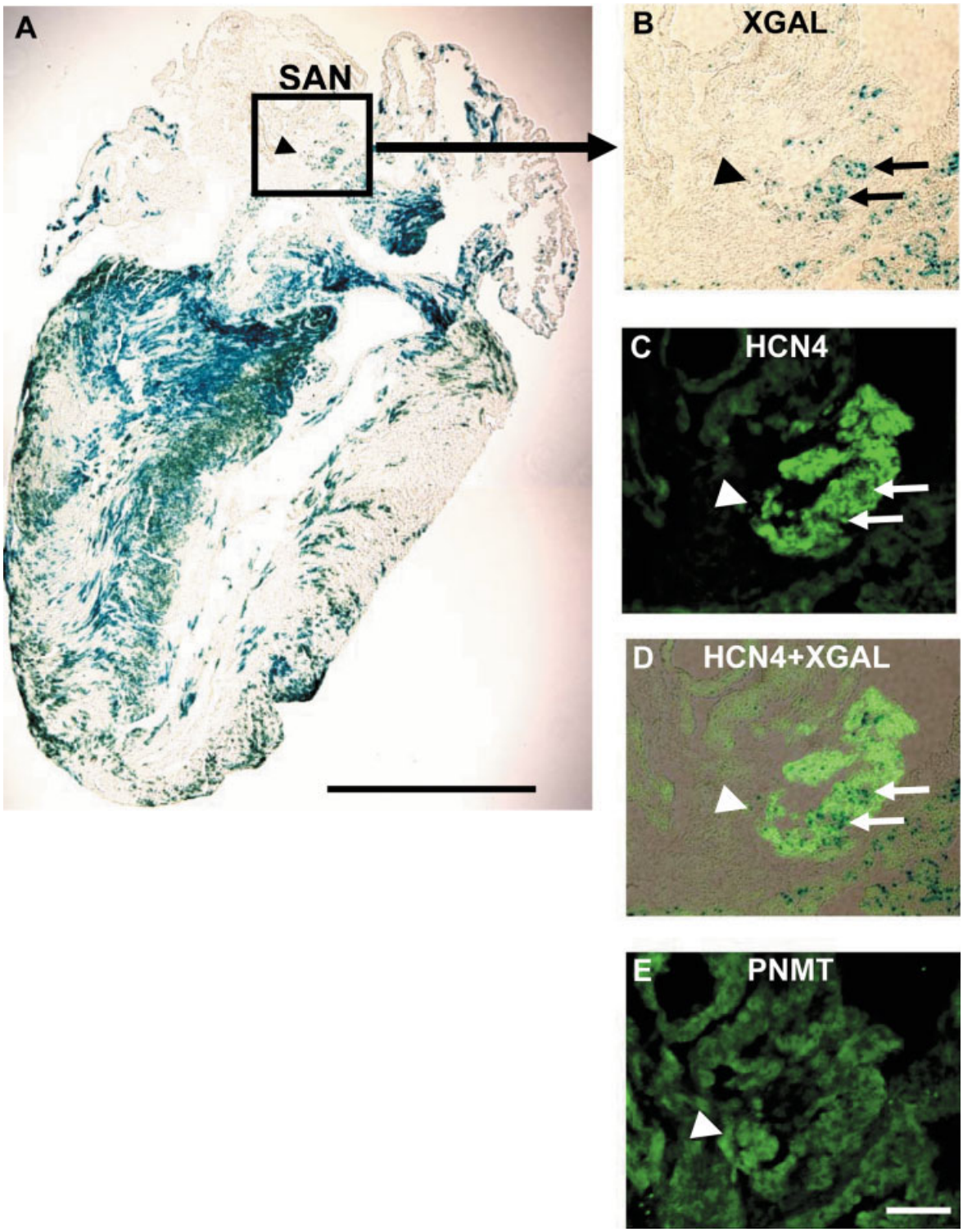

Fig. 8. LacZ expression patterns in neonatal mouse heart sinoatrial node (SAN) region. **A:** Low-magnification (×4 objective) frontal view of an XGAL-stained Pnmt-Cre/R26R heart section at postnatal day 2. The SAN region is boxed. B–E: Higher-magnification (×20 objective) view of the boxed region from A. **B:** Brightfield image of blue XGAL-stained cells in the SAN region. **C:** HCN4 immunofluorescent (green) staining of the same section shown in B. **D:** Overlay image of B and C. **E:** Pnmt immunofluorescent (green) staining of an equivalent region to that shown in B–D from an adjacent section. Arrowheads point to the equivalent region in each panel where $Pnmt^{+}$ cells were found. Arrows in C and D indicate examples of pacemaker cells costained for HCN4 and XGAL. Pnmt, phenylethanolamine n-methyltransferase. Scale bar = 1.0 mm in A, 0.1 mm in E (applies to B–E).

tricular septum, especially along the crest and the descending lateral branches, is consistent with the expected pattern of ventricular conduction system myocytes (Viragh and Challice, 1977; Moorman et al., 1998; Rentschler et al., 2001).

LacZ expression in Pnmt-Cre/R26R embryonic mouse hearts was definitely not confined to the pacemaking and conduction systems. In fact, the vast majority of cardiac cells derived from Pnmt-expressing precursors appear to be nonpacemaking myocytes. At present, there is no evidence to suggest that Pnmt-expressing cells give rise to nonmyocardial cells within the heart, but further costaining experiments with additional cell-specific markers (e.g., for fibroblasts, smooth muscle, neuronal, endocardial, and epicardial cells) needs to be performed in this mouse model before such a determination can be made. This caveat notwithstanding, our data suggest that Pnmt is a novel marker for a subpopulation of developing myocytes in the heart. Cardiac cells that express Pnmt may ultimately become working myocardial cells in both atria and ventricles as well as in specialized myocytes constituting the cardiac pacemaking and conduction systems.

EXPERIMENTAL PROCEDURES

Creation of Pnmt-Cre Knock-In/Knockout Mice

To construct targeting vector pKP506, we first isolated and subcloned a 7-kb *Sac*I fragment from bacterial artificial chromosome 238M20 (Genome Systems). This fragment carries Pnmt exon 1 and includes 3.3 kb upstream of the ATG initiation codon and also 3.7 kb of sequences 3′ of the translation start site. A 1.4-kb *Sex*AI fragment carrying exon 1 was next subcloned and mutagenized by using the Gene Editor Mutagenesis Kit (Promega) to add a unique *Eco*RI site in place of the normal Pnmt translation initiation codon. A cassette carrying the Cre-recombinase gene fused to a nuclear localization signal was then inserted at this unique *Eco*RI site so that the expected mRNA product is a fusion of the Pnmt 5′ untranslated leader to sequences encoding the Cre-recombinase protein. The cassette also included Neo^R sequences flanked by FRT recombination sites. This modified *Sex* AI fragment was then exchanged with its wild-type cognate on the *Sac*I clone. Finally the diphtheria toxin A gene was added adjacent to the 5′ Pnmt flank for negative selection.

Forty-five micrograms of linearized vector DNA were electroporated into RI mouse embryonic stem cells. G418-resistant clones were isolated and their DNAs characterized by Southern blotting using probes external to the targeting vector (Fig. 1). Cells from two positive clones were injected into C57BL/6 blastocysts and chimeric mice from these injections were mated to C57BL/6 females. Genotypes at the Pnmt locus were identified by PCR analysis by using the following primers: primer 21, 5′-CAG GCG CCT CAT CCC TCA GCA GCC-3′; primer 22, 5′-CTG GCC AGC GTC GGA GTC AGG GTC-3′; and primer 23, 5′-GGT GTA CGG TCA GTA AAT TGG ACA CCG TCC TC-3′. These amplification reactions yield products of 200 and 160 bp for the wild-type and the mutant alleles, respectively. $Pnmt^{Cre/+}$ mice were then intercrossed or mated to R26R reporter mice as described in the text.

Catecholamine Radioimmunoassays

Epinephrine and norepinephrine concentrations were measured by radioimmunoassay as described previously (Ebert and Thompson, 2001). Briefly, adrenal glands were isolated from decapitated neonates and immediately frozen on dry ice. Individual adrenal gland extracts were prepared by sonication for 10 sec in 0.1 M HCl, followed by microcentrifugation (14,000 $\times$ *g*, 10 min) to remove residual debris. The extracts were assayed using a commercially available radioimmunoassay (ALPCO Labs, Inc., Wyndham, NH), and protein concentrations were determined by using the Bio-Rad (Hercules, CA) protein assay. Equivalent amounts of protein (5 ng/sample) were assayed in a volume of 0.25 ml. Results are expressed as mean $\pm$ SEM and compared for statistically significant differences by one-way analysis of variance with $P < 0.05$ required to reject the null hypothesis.

Whole-Mount Staining for β-Galactosidase Activity

Embryos were staged by timed matings. Females carrying a vaginal plug were removed from the mating cage, and noon of that day was considered to be E0.5. Isolated embryos were fixed 50 min at 4°C in PBS containing 2% paraformaldehyde (w/v) and 2% glutaraldehyde (v/v). Embryos were rinsed at 4°C with phosphate buffered saline (PBS) three times for 30 min each and then incubated in PBS containing 1 mg/ml XGAL (5-bromo-4-chloro-3-indoyl-beta-D-pyranoside), 5 mM ferricyanide, 5 mM ferrocyanide, 2 mM $MgCl_2$, and 0.2% Ipegal CA-630 (Sigma). After 15 hr at 30°C, the embryos were rinsed in PBS containing 3% dimethyl sulfoxide and then stored at 4°C in PBS.

Immunofluorescent Histochemical Staining

Coimmunofluorescent histochemical staining was performed essentially as described previously (Ebert and Thompson, 2001). Primary antibodies used in this study include rabbit polyclonal antibodies from Chemicon International (Temecula, CA) that selectively recognize either Pnmt (AB110) or HCN4 (AB5808) and mouse monoclonal antibodies from Sigma-Aldrich (St. Louis, MO) that selectively recognize either Th (T1299) or sarcomeric α-actinin (A7811). Fluorescently tagged secondary antibodies were obtained from Jackson Immunolabs (Denver, PA), and include fluorescein isothiocyanate–conjugated donkey anti-rabbit IgG and Texas Red–conjugated donkey anti-mouse IgG. All antibodies were used at 1:100 dilution, except for the anti-HCN4 antibody, which was used at 1:50 dilution.

Embryos were isolated from timed-pregnant females and fixed with freshly prepared 4% paraformaldehyde in 0.1 M PBS, pH 7.3 for 1–2 hr on

ice. The samples were then transferred to 30% sucrose solution in PBS, pH 7.3, and allowed to equilibrate at 4°C for at least 48 hr. The sucrose-saturated samples were then shipped to FD Neurotechnologies, Inc. (Catonsville, MD) for sectioning (20 μm) and mounting onto Super-Frost Plus microscope slides (Fisher Scientific, Inc., Pittsburgh, PA). The sections were then frozen and stored at −80°C for subsequent use.

For experiments where XGAL staining and immunofluorescent labeling were combined, we first performed the XGAL staining on the sections overnight as described above. The XGAL solution was then removed, and the sections were washed with PBS (3 × 10 min each) before initiating the immunofluorescent staining as described in the preceding paragraph. Digital images were collected by using a Nikon Eclipse E1000 fluorescence microscope and processed for display by using Adobe Photoshop 5.5 software.

REFERENCES

Anderson DJ. 1993. Molecular control of cell fate in the neural crest: the sympathoadrenal lineage. Annu Rev Neurosci 16:129–158.

Armstrong DM, Ross CA, Pickel VM, Joh TH, Reis DJ. 1982. Distribution of dopamine-, noradrenaline-, and adrenaline-containing cell bodies in the rat medulla oblongata: demonstrated by the immunocytochemical localization of catecholamine biosynthetic enzymes. J Comp Neurol 212:173–187.

Bohn MC. 1983. Role of glucocorticoids in expression and development of phenylethanolamine N-methyltransferase (PNMT) in cells derived from the neural crest: a review. Psychoneuroendocrinology 8:381–390.

Bohn MC, Goldstein M, Black IB. 1986. Expression and development of phenylethanolamine N-methyltransferase (PNMT) in rat brain stem: studies with glucocorticoids. Dev Biol 114:180–193.

Claycomb WC. 1976. Biochemical aspects of cardiac muscle differentiation. Possible control of deoxyribonucleic acid synthesis and cell differentiation by adrenergic innervation and cyclic adenosine 3′:5′-monophosphate. J Biol Chem 251:6082–6089.

Claycomb WC. 1977. Cardiac-muscle hypertrophy. Differentiation and growth of the heart cell during development. Biochem J 168:599–601.

Cooper J, Bloom F, Roth R. 1991. Norepinephrine and epinephrine. The biochemical basis of neuropharmacology. New York: Oxford University Press. p 220–284.

Coupland RE, Tomlinson A. 1989. The development and maturation of adrenal medullary chromaffin cells of the rat in vivo: a descriptive and quantitative study. Int J Dev Neurosci 7:419–438.

de la Cruz MV, Sanchez GC, Arteaga MM, Arguello C. 1977. Experimental study of the development of the truncus and the conus in the chick embryo. J Anat 123:661–686.

Ebert SN, Thompson RP. 2001. Embryonic epinephrine synthesis in the rat heart before innervation: association with pacemaking and conduction tissue development. Circ Res 88:117–124.

Ebert SN, Baden JM, Mathers LH, Siddall BJ, Wong DL. 1996. Expression of phenylethanolamine n-methyltransferase in the embryonic rat heart. J Mol Cell Cardiol 28:1653–1658.

Garcia-Frigola C, Shi Y, Evans SM. 2003. Expression of the hyperpolarization-activated cyclic nucleotide-gated cation channel HCN4 during mouse heart development. Gene Expr Patterns 3:777–783.

Hammang JP, Bohn MC, Messing A. 1992. Phenylethanolamine N-methyltransferase (PNMT)-expressing horizontal cells in the rat retina: a study employing double-label immunohistochemistry. J Comp Neurol 316:383–389.

Hoffman B. 2001. Catecholamines, sympathetic drugs, and adrenergic receptor antagonists. In: Hardman J, Limbird L, editors. Goodman & Gilman's The pharmacological basis of therapeutics. New York: McGraw-Hill. p 215–268.

Huang MH, Friend DS, Sunday ME, Singh K, Haley K, Austen KF, Kelly RA, Smith TW. 1996. An intrinsic adrenergic system in mammalian heart. J Clin Invest 98: 1298–1303.

Ignarro LJ, Shideman FE. 1968. Appearance and concentrations of catecholamines and their biosynthesis in the embryonic and developing chick. J Pharmacol Exp Ther 159:38–48.

Jiang X, Rowitch DH, Soriano P, McMahon AP, Sucov HM. 2000. Fate of the mammalian cardiac neural crest. Development 127:1607–1616.

Kelly RG, Buckingham ME. 2002. The anterior heart-forming field: voyage to the arterial pole of the heart. Trends Genet 18:210–216.

Kelly RG, Brown NA, Buckingham ME. 2001. The arterial pole of the mouse heart forms from Fgf10-expressing cells in pharyngeal mesoderm. Dev Cell 1: 435–440.

Kirby M. 1999. Contribution of neural crest to heart and vessel morphology. In: Harvey R, Rosenthal N, editors. Heart development. San Diego: Academic Press. p 179–193.

Kopp N, Denoroy L, Renaud B, Pujol JF, Tabib A, Tommasi M. 1979. Distribution of adrenaline-synthesizing enzyme activity in the human brain. J Neurol Sci 41:397–409.

Mjaatvedt CH, Nakaoka T, Moreno-Rodriguez R, Norris RA, Kern MJ, Eisenberg CA, Turner D, Markwald RR. 2001. The outflow tract of the heart is recruited from a novel heart-forming field. Dev Biol 238:97–109.

Moorman A, de Jong F, Denyn M, Lamers W. 1998. Development of the cardiac conduction system. Circ Res 82:629–644.

Rentschler S, Vaidya DM, Tamaddon H, Degenhardt K, Sassoon D, Morley GE, Jalife J, Fishman GI. 2001. Visualization and functional characterization of the developing murine cardiac conduction system. Development 128:1785–1792.

Sawchenko PE, Bohn MC. 1989. Glucocorticoid receptor-immunoreactivity in C1, C2, and C3 adrenergic neurons that project to the hypothalamus or to the spinal cord in the rat. J Comp Neurol 285:107–116.

Soriano P. 1999. Generalized lacZ expression with the ROSA26 Cre reporter strain. Nat Genet 21:70–71.

Stieber J, Herrmann S, Feil S, Loster J, Feil R, Biel M, Hofmann F, Ludwig A. 2003. The hyperpolarization-activated channel HCN4 is required for the generation of pacemaker action potentials in the embryonic heart. Proc Natl Acad Sci U S A 100:15235–15240.

Thomas SA, Matsumoto AM, Palmiter RD. 1995. Noradrenaline is essential for mouse fetal development. Nature 374: 643–646.

Viragh S, Challice CE. 1973. Origin and differentiation of cardiac muscle cells in the mouse. J Ultrastruct Res 42:1–24.

Viragh S, Challice C. 1977. Development of the conduction system in the mouse embryo heart II. Histogenesis of the atrioventricular node and bundle. Dev Biol 56:397–411.

Waldo KL, Lo CW, Kirby ML. 1999. Connexin 43 expression reflects neural crest patterns during cardiovascular development. Dev Biol 208:307–323.

Waldo KL, Kumiski DH, Wallis KT, Stadt HA, Hutson MR , Platt DH, Kirby ML. 2001. Conotruncal myocardium arises from a secondaryheartfield.Development128: 3179–3188.